NONCOMMUTING FILTERS AND DYNAMIC MODELLING FOR LES OF TURBULENT COMPRESSIBLE FLOW IN 3D SHEAR LAYERS

B. GEURTS, B. VREMAN, H. KUERTEN AND R. VAN BUUREN
Department of Applied Mathematics, University of Twente
P.O. Box 217, 7500 AE Enschede, The Netherlands

Abstract. Large-eddy simulation of complex turbulent flows involves the filtering and modelling of small scale flow structures whose intensity shows large spatial variations in the flow domain. This suggests the use of filters with nonuniform filterwidth. Such filters fail to commute with spatial derivatives and give rise to additional 'noncommutation' terms in LES. We construct higher order filters and show that the subgrid terms and the new noncommutation terms are *a priori* of comparable magnitude. We apply these filters to DNS data of the temporal mixing layer. The magnitude of the noncommutation terms and their contribution to the kinetic energy dynamics is determined. Finally, we show that LES predictions significantly depend on the specific explicit filter used in dynamic subgrid modelling.

1. Introduction

The numerical simulation of transitional and turbulent flow forms a field of considerable interest (Kleiser and Zang, 1991). Through continuous advances in computing capabilities, direct numerical simulation (DNS) of transitional and low-Reynolds turbulent flow in simple geometries has become feasible. This requires the detailed spatial and temporal resolution of all relevant scales of motion. Restrictions arising from available computing capabilities render DNS impossible for practically relevant configurations at high Reynolds numbers. Thus, modelling of the governing equations, which reduces the degrees of freedom of the dynamical system, is required. For this purpose the central first step consists of an averaging of the Navier-Stokes equations. A detailed modelling is obtained in Large-Eddy Simulation (LES) which can be obtained from the Navier-Stokes equations through

the application of a spatial filter. In the derivation of the LES equations one commonly adopts a convolution filter which has the property that filtering and partial differentiation can be interchanged. In that case the effect of the filtering is restricted to the appearence of so called subgrid scale terms and the resulting equations can be written in conservative form. A large drawback of convolution filters, however, is the fact that the filter-width is constant. This complicates the extension of the LES approach to complex geometries for which a varying filterwidth is required in view of the strong spatial variations in the small scale turbulence intensities. However, a nonuniform filterwidth gives rise to additional 'noncommutation' terms in the filtered equations (Geurts *et al.*, 1994; Ghosal and Moin, 1995; van der Ven, 1995).

The higher order compact support filters developed in this paper are obtained by requiring invariance of polynomials up to a certain order. The 'noncommutation' properties of these filters will be investigated and it will be shown that the common subgrid-terms and the noncommutation terms are in general of comparable magnitude. Apart from a varying filterwidth, these filters are characterized by their 'skewness'. Through an application of these filters to DNS-data for the compressible mixing layer *a priori* estimates are obtained for the different contributions to the LES equations for varying grid nonuniformity. Whereas the turbulent stress tensor has a predominant dissipative contribution to the dynamics of the kinetic energy the noncommutation terms also contribute to backscatter. Finally, we consider the influence of the specific realization of the explicit filtering in dynamic subgrid modelling and compare simulation results obtained with the dynamic eddy viscosity model and the dynamic mixed model.

The organization of this paper is as follows. In section 2 we introduce higher order compact support filters and study their noncommutation properties. Section 3 is devoted to *a priori* evaluation of the magnitude and effects of the noncommutation terms compared to the common subgrid terms for the mixing layer. In section 4 we present LES results for the mixing layer showing the influence of a higher order realization of the explicit filtering in the dynamic modelling. We summarize our findings in section 5.

2. Higher order non-commuting filters

In this section we introduce higher order filters and study their commutation properties in one spatial dimension. The consequences of the realizability conditions on the filters are established and the effects related to the 'skewness' of the filter are illustrated with a Fourier analysis.

We consider a signal $f : I\!R \to I\!R$ and define the filter operation $f \to \overline{f}$

by:

$$\overline{f}(x) = \int_{x-\Delta_-(x)}^{x+\Delta_+(x)} \frac{\mathcal{H}(x,\xi)}{\Delta(x)} f(\xi)d\xi \tag{1}$$

in which Δ_+, $\Delta_- \geq 0$ denote the x-dependent upper- and lower filterwidths respectively, $\Delta = \Delta_+ + \Delta_- > 0$ is the filterwidth and $\mathcal{H}/\Delta$ the filter-kernel. We arrive at a more convenient formulation after a change of coordinates in which we put $y = (\xi - x)/\Delta(x)$. This leads to:

$$\overline{f}(x) = \int_{I_x} \mathcal{H}(x, x + \Delta(x)y)f(x + \Delta(x)y)dy \tag{2}$$

where $I_x = [(s(x)-1)/2, (s(x)+1)/2]$. Here we introduced the 'normalized skewness' $s(x) = S(x)/\Delta(x)$ in terms of the skewness $S(x) = \Delta_+(x) - \Delta_-(x)$. We introduce N-th order filters by requiring:

$$\int_{I_x} \mathcal{H}(x, x + \Delta(x)y)y^k dy = \delta_{k0} \quad ; \quad k = 0, 1, .., N - 1 \tag{3}$$

in which δ_{ij} denotes the Kronecker delta. These filters have the property that $\overline{P_{N-1}}(x) = P_{N-1}(x)$ for any polynomial P of order $N - 1$. Application of this filter to the M-th order Taylor expansion of f around x yields:

$$\overline{f}(x) = f(x) + \sum_{k=N}^{M-1} \left(\Delta^k(x)M_k(x)\right) f^{(k)}(x) + \Delta^M(x)R_M(f) \tag{4}$$

where $f^{(k)}$ denotes the k-th derivative of f and we introduced

$$M_k(x) = \frac{1}{k!} \int_{I_x} \mathcal{H}(x, x + \Delta(x)y)y^k dy \tag{5}$$

Moreover, $R_M(f)$ denote the rest-term. Hence, if $M > N$ the leading order term of $\overline{f} - f$ scales with Δ^N. For notational convenience we will not denote the explicit x-dependence in the sequel and we ignore the rest-terms.

The effect of the filter-operation on the signal f as expressed in (4) can straightforwardly be extended to derivatives of f and to nonlinear operations g on the signal. These expressions can be used in order to derive the basic noncommutation properties. For N-th order filters the commutator with differentiation can be written as:

$$\overline{f'} - \overline{f}' = -\sum_{k=N}^{M-1} \left(\Delta^k M_k\right)' f^{(k)} + ... \tag{6}$$

in which the dots denote higher order terms in Δ. This commutator is written in the usual way in terms of higher order derivatives of f where

now a factor $(\Delta^k M_k)'$ appears. In general it is quite complicated to obtain detailed estimates for this term. Using the definition of the filter (1) and some partial integration one may distinguish two contributions, one due to x-dependence of $\Delta_\pm$ and one from the fact that the filter-kernel is not of convolution type which results in a contribution containing $\partial_x \mathcal{H} + \partial_\xi \mathcal{H}$.

Another commutator which is relevant for filtering nonlinear terms arises when the filter-operation is combined with an algebraic operation on the signal: $\overline{(g \circ f)} - (g \circ \overline{f})$. An important example of such a nonlinearity is $g(z) = z^2$. For this particular example we obtain:

$$\overline{f^2} - \overline{f}^2 = \sum_{k=N}^{M-1} (\Delta^k M_k) \left((f^2)^{(k)} - 2ff^{(k)} \right) - (\overline{f} - f)^2 + \dots \qquad (7)$$

The scaling with Δ^N is readily verified for $N > 1$. In case $N = 1$ the lowest order term in the summation equals 0 since $(f^2)' = 2ff'$ and the commutator scales with Δ^2 with contributions from the term $k = 2$ in the summation and an additional contribution from $(\overline{f} - f)^2$. In the Navier-Stokes equations the latter commutator arises inside a divergence operator which gives rise to a term $\sim \Delta^{N-1}$, i.e. comparable to the commutator with first order derivatives. Hence, there is *a priori* no justification to ignore the latter terms while retaining the common subgrid-terms, which is in contrast with the findings in (van der Ven, 1995). Of course the actual magnitude of the noncommutation with differentiation also depends on the spatial variation of $\Delta(x)$ and $s(x)$ which may reduce the magnitude considerably. Moreover, the effect on the evolution of the solution arising from the various noncommutation terms can be quite different.

The construction of specific higher order filters relies on a Taylor expansion of the filter-function $\mathcal{H}$. In the definition of the filter-operation (1) the filter-function $\mathcal{H}$ is required for ξ in a neighborhood of x:

$$\mathcal{H}(x, \xi) = \mathcal{H}(x, x) + \sum_{m=1}^{N-1} \frac{\partial_\xi^{(m)} \mathcal{H}(x, x)}{m!} (\xi - x)^m + \dots \qquad (8)$$

in which $\partial_\xi^{(m)} \mathcal{H}(x, x)$ denotes the m-th partial derivative of $\mathcal{H}(x, \xi)$ with respect to ξ evaluated at $\xi = x$. With this filter we arrive at

$$(\Delta^k M_k) = \frac{\Delta^k}{k!} \sum_{m=0}^{L-1} \frac{\Delta^m \partial_\xi^{(m)} \mathcal{H}(x, x)}{m!} \int_{I_x} y^{m+k} dy + \dots \qquad (9)$$

The definition of N-th order filters as given in (3) can also be expressed as $(\Delta^k M_k) = \delta_{k0}$ for $k = 0, 1, .., N - 1$. Thus the truncated polynomial representation of N-th order filter satisfies a linear system of equations

from which the required $\Delta^m \partial_\xi^{(m)} \mathcal{H}$ follow. We can specify the form of the filter-function conveniently as $\mathcal{H}(x,\xi) = \mathcal{G}(s,y)$. In view of the symmetries it appears that $\mathcal{G}(-s,y) = \mathcal{G}(s,-y)$ for $y \in I_x$ and in particular that $\mathcal{G}(0,y)$ is an even function of y. This implies that the $(2N-1)$-th and the $(2N)$-th order filters coincide if $s = 0$.
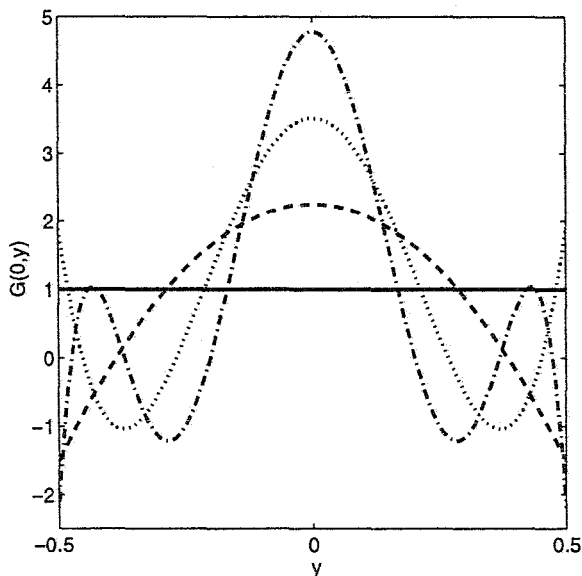

Figure 1. The filter-kernels $\mathcal{G}_N$ for symmetric higher-order filters, i.e. $s = 0$. The results for $N = 1$ (solid); $N = 3$ (dashed); $N = 5$ (dotted) and $N = 7$ (dash-dotted) are shown. Notice $\mathcal{G}_{2N} = \mathcal{G}_{2N-1}$ for symmetric filters.

In figure 1 we plotted the filter-kernels $\mathcal{G}_N$ at $s = 0$. In (Vreman *et al.*, 1994a) it was shown that the realizability conditions for the turbulent stress tensor are satisfied if and only if the kernel is positive. The explicit filters plotted above, however, show filter-kernels which are not strictly positive in case $N \geq 3$. Also, the $N = 2$ kernel is positive only if $|s| < 1/3$. Hence, only first or second order filters are allowed if the turbulent stress tensor should be realizable and the normalized skewness may not exceed $1/3$ for second order filters.

So far we considered the effect of applying an N-th order filter to a signal which can be represented by a Taylor-expansion. As long as the higher order contributions to $\overline{f} - f$ are small we obtain an accurate representation of $\overline{f}$. However, for very rapidly fluctuating signals on a scale comparable to Δ this approximation is no longer adequate. In order to analyze this we focus on the filtering of $\sin(kx)$ for which

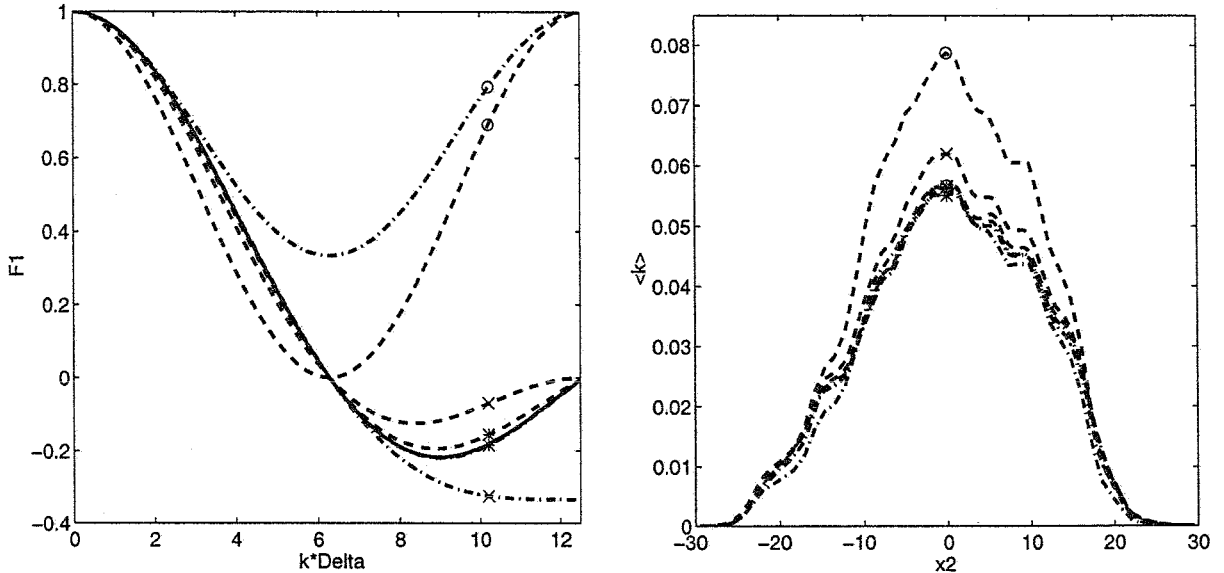$$\overline{\sin(kx)} = F_1(s, k\Delta) \sin(kx) + F_2(s, k\Delta) \cos(kx) \qquad (10)$$

Figure 2. The numerical approximation to F_1 of the symmetric top-hat filter (solid) with the composite trapezoidal rule (dashed) and the composite Simpson rule (dash-dotted) (left). The turbulent kinetic energy profiles $< k >$ (right) evaluated at $t = 100$. We used $\Delta = 2h$, $\Delta = 4h$ and $\Delta = 8h$ marked with 'o', 'x' and '*' respectively.

where we introduced the 'characteristic filter-functions':

$$F_1(s, k\Delta) = \int_{I_x} G(s, y) \cos(k\Delta y) dy \quad ; \quad F_2(s, k\Delta) = \int_{I_x} G(s, y) \sin(k\Delta y) dy$$

$$(11)$$

Notice that $F_2(0, k\Delta) = 0$ and the only effect of symmetric filters is an amplitude change. This also shows that skewness of the filter contributes to a phase-shift in the filtered signal. Further analysis of F_1 and F_2 for different filters and skewness shows that the higher order filters can even increase the amplitude of rapidly oscillating signals on a length-scale comparable to Δ, and only effectively reduce the signal as $k\Delta \gg 1$. An analysis of the effect of N-th order filters on stochastic signals could be interesting in the context of LES. Moreover, the influence of the skewness on the models for the subgrid-terms requires further attention.

3. A priori evaluation of noncommutation terms

In this section we formulate the higher order filters in a numerically consistent way using Newton-Cotes integration and apply these filters to DNS data obtained for the temporal compressible mixing layer at convective Mach-number $M = 0.2$ and Reynolds number $Re = 100$ based on the initial vorticity thickness (Vreman *et al.*, 1995).

In order to arrive at a numerically consistent representation of the filters introduced in the previous section the numerical integration should be sufficiently accurate in order to maintain the basic invariance prop-

erties of these filters. The discrete data $\{f_j\}$ are assumed to be represented on a grid $\{x_j\}$. In order to define the filter we adopt the following definition for the filterwidth and the skewness: $\Delta(x_i) = x_{i+n_+} - x_{i-n_-}$; $S(x_i) = x_{i+n_+} - 2x_i + x_{i-n_-}$ where $n_\pm \geq 0$ specify the upper and lower filterwidth distributions on the grid. The numerical filtering should be such that invariance of x^α, $\alpha = 0, .., N - 1$ is maintained. Within the framework of Newton-Cotes integration such integration rules can readily be specified, also in composite form. If $n_\pm$ are small the numerical filtering is quite different from the analytical filtering. Numerical filtering of $\sin(kx)$ using the symmetric top-hat filter and the (composite) trapezoidal and Simpson rules at different values of $n_\pm$ is shown in figure 2. As $n_\pm = 1$, the numerical filtering of the small scale structures differs considerably from the analytic filtering. The use of Simpson integration instead of the trapezoidal rule leads to less reduction of the small scale structures which is also illustrated in the profiles of the turbulent kinetic energy $< k >$ shown in figure 2 which are lower in case Simpson integration is adopted.

We proceed with the filtering of the Navier-Stokes equations and use DNS-data obtained from the temporal compressible mixing layer on a uniform grid with 192^3 grid-cells. The evolution of the flow displays four large rollers at $t = 20$ which subsequently interact and give rise to two spanwise rollers at $t = 40$ and one large roller with many small-scale structure at $t = 80$. A mixing transition to turbulence arises in this flow.
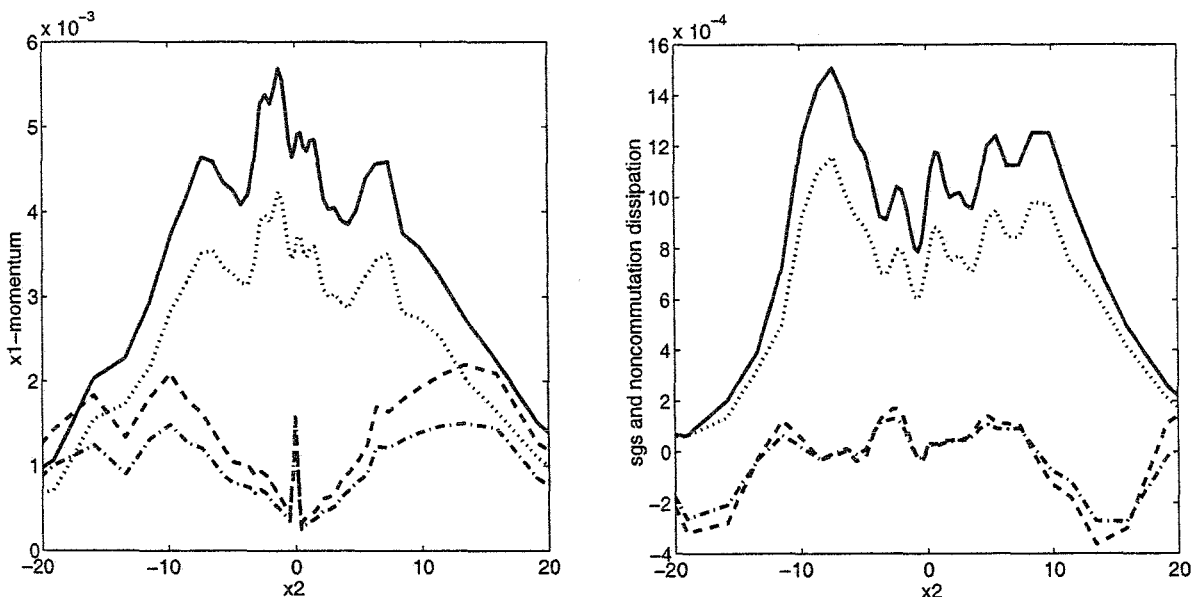

Figure 3.   Discrete L_2-norm of the subgrid (T: solid, S: dotted) and noncommutation term (T: dashed, S: dash-dotted) in the x_1-momentum equation (left). Contribution to the kinetic energy dynamics from the turbulent stress tensor (T: solid, S: dotted) and due to the noncommutation term (T: dashed, S: dash-dotted). The data at $t = 100$ and $a = 0.2$ are shown on the 48^3 grid after averaging over the homogeneous directions.

In order to evaluate the effects of the filtering the data have been trans-

ferred to a grid which is nonuniform in the (normal) x_2 direction only. For the nonuniform grid we use the mapping

$$x_2 = \frac{1}{2} L_2 \frac{a\eta}{1 + a - \eta} \qquad (12)$$

to generate the positive x_2-nodes and we complete this grid by reflection in $x_2 = 0$. Here η is in $[0, 1]$, L_2 denotes the extent in the x_2 direction and the parameter a controls the grid-nonuniformity. The original data on the uniform grid have been transferred to the nonuniform grid by using fourth order accurate interpolation. In the sequel we consider a coarse grid with 48^3 grid-cells, an intermediate grid with 96^3 grid-cells and a fine grid with 192^3 grid-cells. On the coarse, intermediate and fine grids we use $n_\pm = 1$, $n_\pm = 2$ and $n_\pm = 4$ respectively. For the filtering in 3D we adopt a 'product-filter' in which the filtering is performed independently in each direction with a 1D filter as described in the previous section.

The effect of the filter is expressed by the following decomposition. Consider a typical convective term in the momentum equations given by:

$$\begin{aligned}
\overline{\partial_j(\rho u_i u_j)} &= \partial_j(\overline{\rho}\tilde{u}_i\tilde{u}_j) \\
&+ [\partial_j(\overline{\rho}(\widetilde{u_i u_j} - \tilde{u}_i\tilde{u}_j))] + [\overline{\partial_j(\rho u_i u_j)} - \partial_j(\overline{\rho\widetilde{u_i u_j}})] \qquad (13)
\end{aligned}$$

where ∂_j denotes the partial derivative with respect to x_j, ρ the density, u_i the velocity in the x_i direction and $(\tilde{\cdot})$ is the Favre filter. The first term on the right hand side corresponds to the mean term, the second is the common turbulent stress term and the last denotes the noncommutation term. Since the grid is nonuniform only in the x_2 direction the noncommutation term is nonzero only if derivatives with respect to x_2 are concerned. As a typical example we show the subgrid and noncommutation terms for $\partial_2(\rho u_1 u_2)$ in figure 3. Use was made of the top-hat filter in combination with trapezoidal (T) and Simpson (S) integration. The noncommutation term is comparable with the turbulent stress term in large parts of the flow domain. Moreover, a definite 'spike' can be seen near $x_2 = 0$ due to a strong local variation of Δ. In order to assess a priori some of the effects of these terms on the dynamics of the kinetic energy we consider the turbulent stress contribution given by $\overline{\rho}\tau_{ij}\partial_j\tilde{u}_i$ where $\tau_{ij} = \widetilde{u_i u_j} - \tilde{u}_i\tilde{u}_j$ and compare this with the contribution arising from the noncommutation term $\tilde{u}_i R_i$ where $R_i = \overline{\partial_j(\rho u_i u_j)} - \partial_j(\overline{\rho\widetilde{u_i u_j}})$ (the summation convention is adopted here). The result is shown in figure 3 from which it becomes clear that the turbulent stress tensor has a dissipative influence. The noncommutation term is considerably lower and can give rise to backscatter.
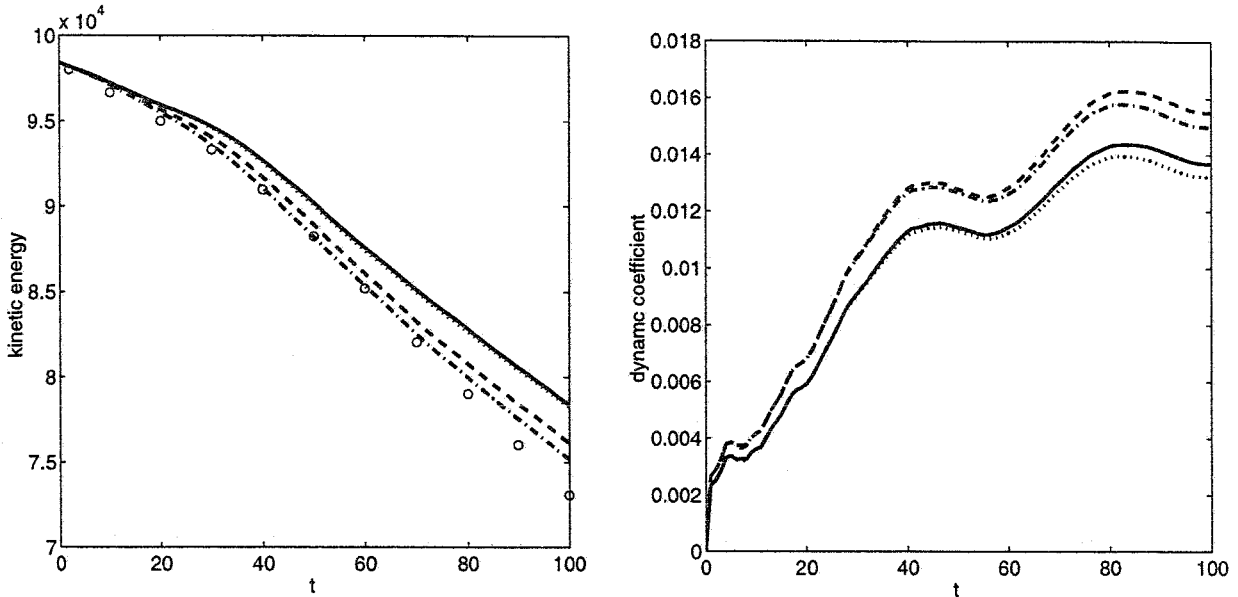
Figure 4. The evolution of the kinetic energy (left): ES (solid); ET (dotted); MS (dashed) and MT (dash-dotted) and the evolution of the dynamic coefficient C_d for the eddy viscosity model (right): SS (solid); ST (dashed); TS (dotted) and TT (dash-dotted). The markers denote the filtered DNS-data.

4. Higher order explicit filtering and dynamic modelling

The formulation of dynamic subgrid models for the turbulent stress tensor implies an explicit filtering of a LES solution. In the previous section we showed that if Δ/h is relatively small the numerical realization of the filter differs significantly from the analytic filter. In this section we show that these differences can contribute also to the simulation results. We concentrate on the top-hat filter and for the numerical realization we compare the use of the trapezoidal rule with Simpson integration using $\Delta = 2h$ in the simulation with a test filter $\Delta = 4h$. The LES results were obtained on a uniform grid with 32^3 grid-cells adopting the dynamic eddy viscosity model (Germano et al., 1991) or the dynamic mixed model (Vreman et al., 1994b). We use the abbreviations E, M for the dynamic eddy viscosity and mixed models. Combination with trapezoidal or Simpson integration is denoted with either T or S.

The formulation of the dynamic models is based on the Germano identity. In this formulation a model coefficient is determined in accordance with the local flow structure. In figure 4 we compare the predictions for the kinetic energy. The influence of the explicit filtering is much larger for the dynamic mixed model compared to the dynamic eddy viscosity model. This directly corresponds to the occurrence of both filters in the formulation of the dynamic mixed model whereas only the $\Delta = 4h$ filter arises in the dynamic eddy viscosity model for which the difference between T and S integration is much smaller. Moreover, in figure 4 the model-coefficient

arising in the dynamic model is shown. Two simulations have been performed; one in which the model is calculated with the trapezoidal rule and one with Simpson integration. During each of these runs the coefficient was also evaluated with the complementary integration rule although this result was not used in the flux-calculation. In the figure these four combinations are labeled AB where A denotes the rule used for the flux and B the rule for the additional evaluation. The result for the model-coefficient C_s shows a decrease in C_s in case Simpson integration is used in the explicit filter. The evaluation of C_s with either the trapezoidal or the Simpson rule is more important than the specific dynamic model used for the flux calculation.

5. Concluding remarks

We presented the construction of higher order noncommuting filters in LES and showed that the contribution of the additional subgrid terms is in general comparable to that of the common subgrid-terms. A numerically consistent formulation of the higher order filters was applied to DNS data of the mixing layer. It was shown that the noncommutation terms can be comparable to the common subgrid terms and the contribution to e.g. the kinetic energy evolution is quite small and contributes to backscatter. The numerical filtering was shown to differ significantly from the analytic filtering in case $\Delta = 2h$. Moreover, the differences between e.g. the trapezoidal and Simpson realization of the filtering were found to be considerable at this Δ/h ratio. In LES the use of dynamic subgrid models for the turbulent stress tensor has given rise to accurate LES predictions for the mixing layer. The specific realization of the explicit filtering which is required in this approach has a large influence on the simulation results for the dynamic mixed model at $\Delta = 2h$.

References

L. Kleiser and T.A. Zang, 'Numerical simulation of transition in wall-bounded shear flows',*Ann. Rev. Fluid Mech.*, **23**, 495, (1991)

B.J. Geurts, A.W. Vreman, J.G.M. Kuerten, 'Comparison of DNS and LES of transitional and turbulent compressible flow: flat plate and mixing layer', AGARD Conf. Proc. 551, 5.1-5-14, Chania, Crete, Greece, (1994)

S. Ghosal, P. Moin, 'The basic equations for the Large Eddy simulation of turbulent flows in complex geometry', *J. Comp. Phys.*, **118**, 24, (1995)

H. van der Ven, 'A family of LES filters with nonuniform filter widths', *Phys. Fluids A*, **7**, 1171, (1995)

A.W. Vreman, B.J. Geurts, J.G.M. Kuerten, 'Realizability conditions for the turbulent stress tensor in Large Eddy Simulation', *JFM*, **278** , 351, (1994a)

A.W. Vreman, B.J. Geurts, J.G.M. Kuerten, 'A priori tests of large eddy simulation of the compressible plane mixing layer', *J.Engg.Math.*, **29**, 299, (1995)

M. Germano, U. Piomelli, P. Moin and W.H. Cabot, 'A dynamic subgrid-scale eddy viscosity model', *Phys. Fluids A*, **3**, 1760, (1991)

A.W. Vreman, B.J. Geurts, J.G.M. Kuerten, 'On the formulation of the dynamic mixed subgrid-scale model', *Phys. Fluids A*, **6**, 4057, (1994b)